Environ. Sci. Technol. **2007**, *41,* 2022−2027

Adsorption of Humic Acid onto Nanoscale Zerovalent Iron and Its Effect on Arsenic Removal

ABUL B. M. GIASUDDIN, SUSHIL R. KANEL, AND HEECHUL CHOI*

Department of Environmental Science and Engineering, Gwangju Institute of Science and Technology (GIST), 1 Oryong-dong, Buk-Gu, Gwangju 500-712, Korea

Batch experiments were performed to investigate the feasibility of humic acid (HA) removal by synthetic nanoscale zerovalent iron (NZVI) and its interaction with As(III) and As(V), the most poisonous and abundant of groundwater pollutants. High-resolution transmission electron microscopy (HR-TEM) and X-ray diffraction (XRD) were used to characterize the particle size, surface morphology of the pristine NZVI and HA-treated NZVI (NZVI-HA), and the zero valence state of the pristine NZVI. It was determined that HA was completely removed by NZVI (0.3 g/L) within a few minutes, at a wide range of initial pH values (∼3.0−12.0). Fourier transform infrared (FTIR) and laser light scattering (zeta potential measurement) studies confirmed that NZVI-HA forms inner-sphere surface complexation at different initial pH conditions. The effects of competing anions showed that there was complete removal of HA in the presence of 10 mM NO^{3-} and SO_4^{2-} whereas HA removal was observed 0%, 18% and 22% in presence of 10 mM $H_2PO_4^{2-}$, HCO_3^- and $H_4SiO_4^0$, respectively. However, the presence of 2 mM Ca^{2+} and Mg^{2+} enhanced HA removal from 17 mg g^{-1} to 76 mg g^{-1} and 55 mg g^{-1}, respectively. Long-term time-resolved studies of XRD and field emission scanning electron microscopy (FE-SEM) with energy-dispersive X-ray (EDX) revealed the formation of various types of new iron oxides (magnetite, maghemite, and lepidocrocites) during the continuous reaction of HA in the presence of water and NZVI at 1, 30, 60, and 90 days. In addition, the surface-area-normalized rate constant (k_{sa}) of adsorption of As(III) and As(V) onto NZVI was reduced in the presence of HA (20 mg L^{-1}), from 100% to 43% and 68%, respectively. Our results show the potential use of NZVI in removing HA and its possible effects on arsenic removal during the application of NZVI in groundwater remediation.

Introduction

Humic substances (HS), a major component of organic matter, are some of the most abundant materials on earth. They are formed during the decomposition of plant and animal biomass in natural systems and usually include a skeleton of alkyl and aromatic units with functional groups such as carboxylic acid, phenolic hydroxyl, and quinone groups attached to them (*1*). These substances commonly range in molecular weight from several hundred to tens of thousands (*2*). Additionally, the presence of HS in natural waters can cause various environmental and health problems including the following: (1) they can cause undesirable color and taste, serving as food for bacterial growth in water distribution systems (*3*); (2) they can bind with heavy metals and biocides to yield high concentrations of these substances and enhance their transport in water (*4*); (3) they can react with chlorine in water treatment to form potentially carcinogenic chlorinated organic compounds, such as trihalomethane (*3*); (4) they can act as a major foulant affecting various applications of membrane processes (*5*); and (5) they have been shown to compete with low-molecular-weight synthetic organic chemicals, as well as inorganic pollutants, reducing their adsorption rates and equilibrium capacities (*6*, *7*). As such, the adsorption of HS has been widely investigated to minimize their impact on the adsorption of other compounds specifically targeted for removal (*8*−*13*).

Micrometer to millimeter-sized zerovalent iron (ZVI) has been used as a permeable reactive barrier (PRB) for groundwater remediation since about 1990. Recently, nanoscale zerovalent iron (NZVI) has been introduced into water treatment processes removing some of the most toxic contaminants with a much higher efficiency than ZVI. These contaminants include arsenic (*14*, *15*), halogenated organic compounds (*16*, *17*), heavy metals (*18*), and nitrates (*19*). Besides its extremely high removal capacity of contaminants in ex-situ conditions and feasibility to create reactive zones, the unique character that makes NZVI of such great interest to environmental scientists and engineers is its applicability in in-situ conditions, with its potential for direct injection into contaminated sites, ultimately acting as a colloidal reactive barrier (CRB) (*20*).

HS exists in natural waters in the range of a few mg/L to a few hundred mg/L C (*2*). Specifically, in Bangladesh and West Bengal, the concentration of HS in groundwater ranges between 1 and 12 mg/L C, where arsenic contamination is the most chronic problem (*21*). When removing pollutants including arsenic, HS may compete with target pollutants and lower its removal efficiency. However, despite the successful application of NZVI in removing various contaminants from the water and soil systems, there have not been extensive studies reporting the adsorption phenomena of HS onto NZVI and its possible impact on NZVI characteristics during the removal of targeted pollutants. As such, to consider the application of NZVI in both ex-situ and in-situ treatment as CRB, a reactive barrier for removing groundwater contaminants, there is an urgent need to investigate the removal capacity of HS and its possible effects on NZVI performance during the removal of other toxic contaminants.

In this paper, we report on humic acid (HA), a representative of HS removal by NZVI, obtaining detailed studies by using different spectroscopic and microscopic techniques, as well as the interaction of HA with arsenic during its removal by NZVI. Our time-resolved long-term study of scanning electron microscopy− energy-dispersive X-ray (SEM-EDX) and X-ray diffraction (XRD) showed chemical and morphological changes of HA and NZVI for up to 3 months. In addition, we tested the influence of HA during the removal of arsenic by NZVI. To this end, the main objectives of our research are (1) to characterize NZVI and its reaction products before and after their reaction with HA, (2) to investigate HA removal by NZVI at different pH conditions and time, (3) to investigate the effect of anions and divalent cations, (4) to present a time-resolved long-term study of HA and NZVI interaction, and (5) to test the influence of HA on the removal of As(III) and As(V) during their removal by NZVI.

* Corresponding author phone: +82-62-970-2441; fax: +82-62-970-2434; e-mail: hcchoi@gist.ac.kr.

10.1021/es0616534 CCC: $37.00
Published on Web 02/17/2007

Experimental Section

Materials and Chemicals. The chemical reagents used in this study, such as $FeSO_4 \cdot 7H_2O$, $NaBH_4$, C_2H_6O, NaOH, HCl, $NaAsO_2$, $Na_2HAsO_4 \cdot 7H_2O$, KI, NaOH, HCl, all anions (NaH_2PO_4, Na_2SiO_3, Na_2SO_4, $NaNO_3$, and $NaHCO_3$), and cations ($CaCl_2 \cdot H_2O$ and $MgCl_2 \cdot 6H_2O$), were reagent grade obtained from Aldrich Chemical Co. and Fluka and were used directly without any pretreatment unless otherwise specified. Leonardite humic acid was obtained from the International Humic Substances Society (IHSS). All chemical stock solutions were prepared using doubly distilled deionized water and were stored at 4 °C. NZVI was synthesized following our previously reported method (*14*). Slight differences from our previous procedure were that 30% ethanol was used instead of 100% water, and $FeSO_4$ was used instead of $FeCl_3$. Synthesized iron nanoparticles were dried at room temperature following the method reported by Nurmi et al. (*22*). Additionally, the characterization of solid-phase NZVI and NZVI-HA products was carried out using XRD, laser light scattering, high-resolution transmission electron microscopy (HR-TEM), SEM-EDX, and a Brunauer-Emmett-Teller (BET) surface area analyzer, as described in our previous report (*14*, *15*).

For Fourier transform infrared (FTIR) samplings, HA was first treated with NZVI for 12 h in different initial pH solutions, and then the treated pH (∼3.0−12.0) solutions were centrifuged and the precipitate was dried at room temperature overnight. FTIR spectra of HA- and NZVI-treated HA complexes were recorded using FTIR (JASCO 460 PLUS spectrometer, Tokyo, Japan) connected with a personal computer. FTIR spectra were measured on KBr pellets prepared by pressing mixtures of 1 mg dry powdered sample and 100 mg spectrometry grade KBr under a vacuum, with precautions taken to avoid moisture uptake.

Batch Experiment for HA Removal. Stock solutions of HA were prepared using 0.5 g HA powder dissolved in 1 L of Deionized water (DI) water followed by filtering the solution through a 0.45-μm membrane filter (cellulose acetate). Batch adsorption studies were conducted in 43-mL lined capped glass bottles (Wheaton) containing 20-mL solutions with varying concentrations of NZVI. The pH of each solution was adjusted using 1 M NaOH and HCl to attain the desired pH value and was measured using an Orion (Model 250A+) pH meter. All HA concentrations were measured with a UV−vis spectrophotometer (UV mini1240) at 254 nm. Concentrations of HA were measured by constructing calibration curves between weight concentrations and the absorbance signal readings. As the UV−vis absorbance of HA is pH-dependent, calibration lines were made for each pH required in the study to convert UV−vis absorbance readings to HA concentration. However, the change in UV−vis absorbance reading with corresponding changes in the solution pH was observed to be insignificant. Additionally, the test solutions were not buffered against pH change to prevent potential interferences, and all adsorption experiments were conducted at room temperature.

Adsorption studies of HA onto NZVI were performed using 20 mg L^{-1} HA treated with varying NZVI solid concentrations (0.1, 0.2, 0.3, 0.5, 1 g L^{-1}) at time intervals of up to 20 min, a duration long enough to reach equilibrium concentrations (Figure 2). Solid NZVI was separated from the solution by centrifugation at 4000 rpm. The final pH was measured, and the supernatants were stored in a refrigerator at 4 °C after filtering in a 0.45-μm membrane filter (cellulose acetate) prior to their analysis. For investigation into the effect of pH, 20 ppm HA was adsorbed on 0.3 g L^{-1} NZVI at various pH ranges (3.0−12.0) after reaction for 12 h; the initial and final pH values were recorded. Furthermore, to investigate the effect of HA on As(III) and As(V) removal kinetics, two sets of batch experiments were performed. In one set, 2 mg L^{-1} As(III) and As(V) solutions without HA were treated with 0.3 g L^{-1} NZVI. In the other set, 2 mg L^{-1} As(III) and As(V) with 20 mg L^{-1} HA solutions were treated with the same amount of NZVI. The experiment was performed at time intervals of up to 30 min. Then, the reaction solutions were filtered and analyzed for As content by hydride generation atomic absorption spectrophotometry (HGAAS; Perkin-Elmer 5100 PC), following the procedure described in our previous report (*14*, *15*).

Anionic and Cationic Effects. Batch tests were performed with competitive anions using 20 mg L^{-1} HA solutions with 0.3 g L^{-1} NZVI in 0.1, 1, and 10 mM concentrations of HCO_3^-, SO_4^{2-}, NO_3^-, $H_4SiO_4^0$, and $H_2PO_4^{2-}$. After a 12-h reaction time, the suspension was centrifuged and filtered through 0.45-μm membrane filters and was analyzed with a UV-spectrometer and was confirmed using a PPM Lab TOC analyzer (PPM Lab Co.). To study the divalent cationic effect, batch tests were performed in two steps. First, 20 ppm HA was treated with 0.2 g L^{-1} NZVI for 12 h; then, in the same solution, between 0.3 and 2.7 mM Ca^{2+} and bteween 0.2 and 2.5 mM Mg^{2+} were separately added. Again, the reaction was performed for 12 h, and the suspension was subsequently centrifuged and filtered through a 0.45-μm membrane filter and was analyzed for HA levels.

SEM and XRD Observation: Long-Term Study. A long-term study was performed by reacting 500 mg L^{-1} HA with 25 g L^{-1} NZVI for 1, 30, 60, and 90 days. Solutions were stirred at 200 rpm and were covered with aluminum foil to prevent photo-oxidation at a controlled room temperature. Each sample was centrifuged, and then the precipitate was freeze-dried and analyzed using field emission scanning electron microscopy (FE-SEM) with EDX and XRD, as described in our previous report (*15*).

Results and Discussion

Characterization of NZVI. Laboratory synthesized iron nanoparticles were analyzed to confirm their nanosize and zero valence states. HR-TEM was then used to investigate the morphology and size distribution of pristine NZVI. Figure 1a shows HR-TEM images of pristine NZVI having very thin layers of oxide shells with distinguishable dark portions inside because of Fe^0 (*15*). NZVI formed a chainlike, aggregated structure because of its natural tendency to remain in a more thermodynamically stable state (*14*). The size distribution histogram (Figure 1b) shows that all the nanoparticles are below 90 nm and that more than 75% of the particles are below 50 nm. XRD (Figure 1c) presents the three major peaks of Fe^0 at 45, 65, and 85 (2-theta degree), consistent with previously reported nano- and microsized zerovalent iron particles (*14*, *22*). The peaks were found to have low intensity because of the presence of an amorphous iron phase (*14*). Pristine NZVI was found to have a specific surface area of 32 $m^2\ g^{-1}$, as measured by a BET surface analyzer, which was a little higher than our previously synthesized NZVI values (24.4 $m^2\ g^{-1}$) (*14*) but similar to other literature values (*16*).

Kinetics of HA Adsorption to NZVI. HA (20 gm L^{-1}) adsorption on NZVI was investigated with different NZVI dosages (0.1, 0.2, 0.3, 0.5, and 1.0 g L^{-1}), at initial pH of 6 (Figure 2). As can be seen, at concentrations of NZVI lower than 0.3 g/L, complete adsorption of HA was not observed over a 20-min period. However, at the concentrations of 0.3 g/L, 0.5 g/L, and 1.0 g/L NZVI, complete adsorption of HA occurred after 20, 10, and 5 min, respectively. Figure 2 (inset) shows that the adsorption of HA on NZVI followed pseudo-first-order reaction kinetics, where K_{obs} is the pseudo-fist-order rate constant of HA.

In the case of micrometer-sized ZVI, this equilibrium time was significantly higher (a few days) (*23*). Moreover, with a further increase of NZVI to 1 g L^{-1}, equilibrium was reached within 5 min. From these time- and dosage-dependent

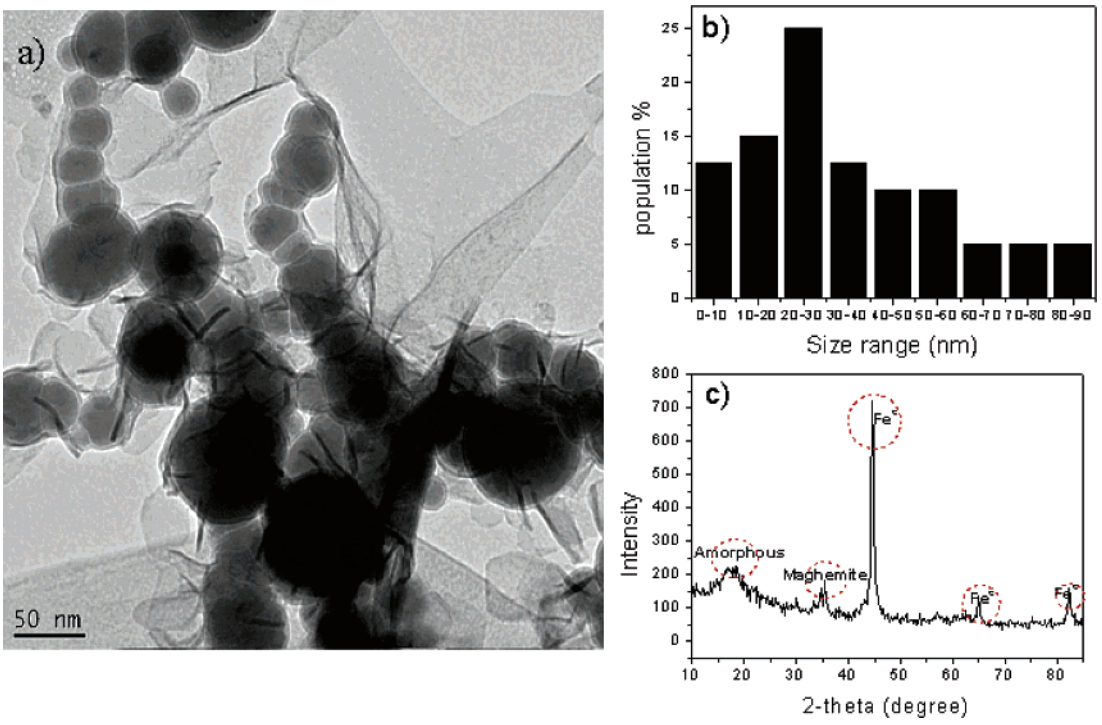

FIGURE 1. TEM image of (a) pristine NZVI, (b) its histogram, and (c) X-ray diffraction analysis of pristine NZVI.

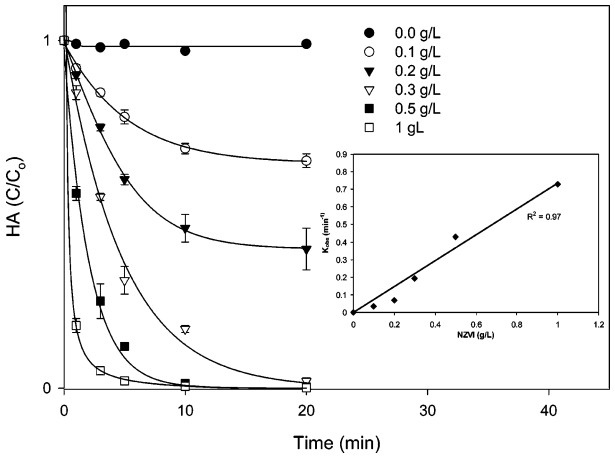

FIGURE 2. Kinetics of HA adsorption onto NZVI. The reaction is pseudo-first-order with respect to the total NZVI concentrations. Reaction conditions: initial HA 20 ppm, 0.01 M NaCl, react for 12 h at 25 °C.

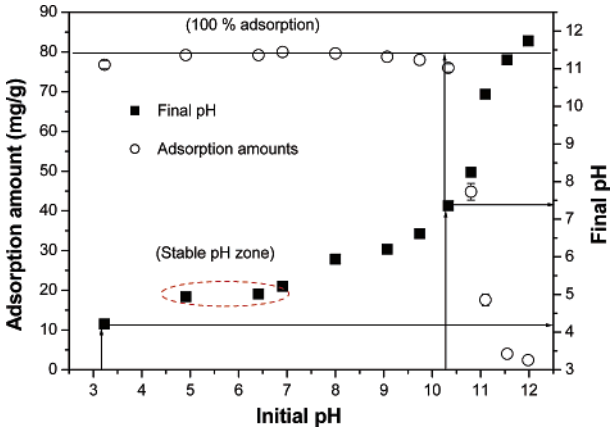

FIGURE 3. Effect of pH on HA adsorption onto NZVI. Reaction conditions: initial HA 20 mg L^{-1}, 0.3 g L^{-1} NZVI, 0.01 M NaCl, react for 12 h at 25 °C.

variations of equilibrium, two important conclusions can be drawn. First, 0.1 g L^{-1} of NZVI does not have enough reactive surfaces to completely adsorb HA, but 0.3 g L^{-1} of NZVI provides an optimum reactive surface for completely adsorbing HA. Second, the decrease of equilibrium time as NZVI dosage increased may be due to two reasons: (a) abundant surface sites for adsorption and (b) reduction of diffusion of HA from the bulk solution to the surface of the NZVI, as the already adsorbed HA showed unfavorable electrostatic interaction charges or repulsion of negative ζ potentials (*24*).

Influence of pH on HA Adsorption. Figure 3 presents the adsorption results of the initial 20 mg L^{-1} HA onto NZVI, with variations in the initial pH and final pH causing corresponding changes in the reacted solution. As can be seen, the maximum adsorption of HA is 80 mg g^{-1} in the pH range 3.0−9.0 and decreases sharply at a pH over 10.0. These results of adsorption patterns of HA on NZVI (Figure 3) are consistent with the electrostatic interaction mechanism, as NZVI remains attractive to negatively charged HA as long as it has a positive charge on its surface. This can be explained by the fact that NZVI became more positively charged as the pH decreased from its point of zero charge at pH 7.7 (*14*). On the other hand, HA has negative charge up to pH > 2.0 (*24*), and NZVI became negatively charged as pH increased, but HA remained negatively charged.

Our results show that the almost complete removal of HA occurred even at an initial pH of 10.0. This may be due to the high protonation of NZVI at higher pH lowering the final pH, which controls the point of zero charge while reacting with HA (*25*). A slight decrease of adsorption rate at pH 3.2 was observed, compared with pH 4.9, possibly because of a small electrostatic repulsion as the dissolved rate of NZVI and HA are opposite to each other when the pH decreases from 4.9 to 3.2 (*25*).

The relationship between the initial and final pH of HA-reacted NZVI (Figure 3) shows that the initial pH of 3.0 increased to 4.3, whereas an initial pH of 10.0 decreased to 7.4. However, with an initial pH of around 5.0−6.5, a stable pH zone was formed because a very insignificant change of pH occurred in that region. This may be due to the continuous

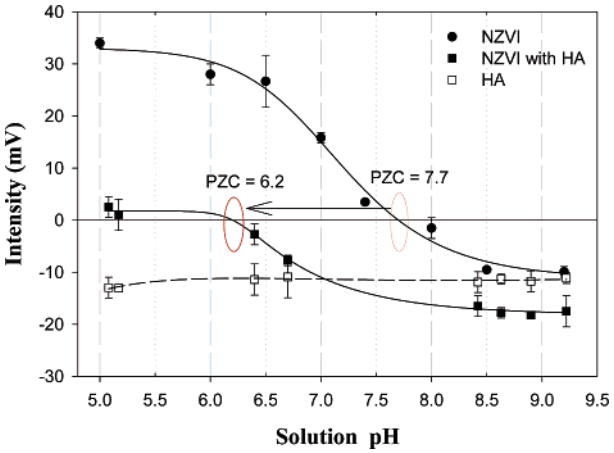

FIGURE 4. Electrophoretic mobility of HA treated and untreated NZVI with respect to pH. Reaction conditions: 0.3 g L^{-1} untreated NZVI, 0.3 g L^{-1} NZVI treated with 20 mg L^{-1} HA in 0.01 M NaCl, 20 ppm HA without NZVI, react for 12 h at 25 °C.

protonation and deprotonation of NZVI in the acidic and basic conditions, as in eqs 1−4. In the pH range 6−11, NZVI initially reacts with H_2O or O_2 to give Fe^{2+} and OH^-; this Fe^{2+} further reacts with H_2O or O_2 or OH^- to precipitate $Fe(OH)_2$ (*14*). Hence, it can be established that an increase or decrease of pH depends on the initial pH of the reacted solution.

$$2Fe^0 + 2H_2O \rightarrow 2Fe^{2+} + H_2 + 2OH^- \quad (1)$$

$$2Fe^0 + O_2 + 2H_2O \rightarrow 2Fe^{2+} + 4OH^- \quad (2)$$

$$6Fe^{2+} + O_2 + 6H_2O \rightarrow 2Fe_3O_4(s) + 12H^+ \quad (3)$$

$$Fe^{2+} + 2OH^- \rightarrow Fe(OH)_2\,(s) \quad (4)$$

The electrophoretic mobility of HA, HA-treated NZVI, and pristine NZVI at different initial pH (5.0−9.3) solutions was measured to determine the point of zero charge (PZC), at which net surface charge is zero. PZC of pristine NZVI and HA-coated NZVI was found to be around 7.7 and 6.2, respectively (Figure 4), whereas HA was negatively charged in the range of 5.0−9.3. In this case, the negatively charged HA adsorbed on NZVI and neutralized the positive charges. As a result, PZC of HA-coated NZVI shifted from 7.7 to 6.2. At pH 5.2, the ζ potential of pristine NZVI surface was 34 mV, which became 5 mV after reaction with HA. Conversely, the ζ potential of pristine NZVI at pH 9 was −12 mV, which changed to −20 mV after reaction with HA. The higher changes of ζ potential at a lower pH, where both inner- and outer-sphere complexations dominate, are consistent with other organic matter sorption onto different iron oxides (*26*, *27*).

FTIR Study of HA Adsorbed onto NZVI. Figure S1 (Supporting Information) shows HA spectra having bands at 2870 cm^{-1} for carboxylate ion stretching; at 2940 cm^{-1} for aliphatic C−H, C−H_2, and C−H_3 stretching; at 1725 cm^{-1} for C═O stretching of carboxylic acids; at 1628 cm^{-1} for C═O stretching vibration of double bonds in ketone and quinone, keton, and quinines; and at 1250 cm^{-1} for C−O stretching of esters, ethers, and phenols (*28*). However, NZVI spectra have bands at 1700−1780 and 2850−3000 cm^{-1}, which may be due to the presence of hydrous components in the oxides. The bands at 915 cm^{-1} may be Fe−O vibrations because of the different stretching patterns in the different crystal phases (*29*). Additionally, when HA reacted with NZVI at different pH values, the complete disappearance of the bands 2870, 2940, and 1725 cm^{-1} in the pH range from 3.23 to 10.8 confirmed that the carboxylate ion, aliphatic C−H, C−H_2, C−H_3, and carboxylic acid took part in the reaction with NZVI by making an inner-sphere complexation with ligand exchange, consistent with previous reports (*30*).

The appearance of new strong bands at 1025 cm^{-1}, representing the C−O stretching of alcoholic compounds, C−O stretching of carbohydrates, and polysaccharide-like substances, implies that a complex chemical reaction occurred between NZVI and HA (*31*). This result was different from the humate−iron complexation in ZVI, where there were no new bands observed. This may suggest that instead of just simple deprotonation of COOH by the ligand exchanges with ZVI species, C−O of esters, ethers, and phenols present in HA more complexation takes place with NZVI (*30*).

Effects of Anionic and Cationic Compounds. Previous reports suggest that oxyanions and divalent cations present in natural water systems could significantly influence the sorption of organic matter (*32*−*36*). Figure S2 (Supporting Information) shows the effects of individual anions (HCO_3^-, SO_4^{2-}, NO_3^-, $H_4SiO_4^0$, and $H_2PO_4^{2-}$) on the adsorption of HA onto NZVI. The NO_3^- and SO_4^{2-} ions at concentrations of up to 10 mM did not affect HA uptake. Similarly, the presence of 0.1 mM anions such as HCO_3^-, $H_4SiO_4^0$, and $H_2PO_4^{2-}$ had no effect on HA adsorption onto NZVI. However, when concentrations were further increased, these anions started reducing the HA adsorption onto NZVI, as HA adsorption was only 20% in the presence of 1 mM $H_2PO_4^{2-}$, and there was no adsorption at 10 mM. On the other hand, 56% and 18% of HA were adsorbed in the presence of 1 mM and 10 mM HCO_3^-, respectively.

In the presence of 10 mM $H_4SiO_4^0$, 22% removal was observed, but no effect was observed in the presence of 1 mM $H_4SiO_4^0$. Furthermore, the presence of NO_3^-, SO_4^{2-} caused no effect on the adsorption capacity of HA on NZVI, which may be due to the enhancement of the reactive sites of the NZVI species (*37*). However, HCO_3^- and $H_2PO_4^{2-}$ were found occupying the reactive surface sites of NZVI to form inner-sphere complexes (*38*). Hence, it could be concluded that $H_4SiO_4^0$, HCO_3^- and $H_2PO_4^{2-}$ compete with HA for sorption sites on NZVI and reduce the adsorption capacity. The high-adsorption tendency of $H_2PO_4^{2-}$ and $H_4SiO_4^0$ onto NZVI has been previously reported where adsorption of inorganic arsenic was significantly reduced because of competitive adsorption with these anions (*14*). However, this is the first report on the influence of anions on HA adsorption during their adsorption onto NZVI.

Figure S3 (Supporting Information) depicts increments of adsorption of HA onto NZVI because of the presence of divalent cations (Ca^{2+} and Mg^{2+}), where HA adsorption capacity increased from 17 mg g^{-1} up to 55 mg g^{-1} and 76 mg g^{-1} because of the presence of 2 mM of Mg^{2+} and Ca^{2+}, respectively. This adsorption enhancement may be due to the compression of the diffuse double layer and charge neutralization of both adsorbate and adsorbent by Ca^{2+} and Mg^{2+} (*35*), as interaction in solutions between salts and organics generally produces a change in the properties of organics. As a result, Ca^{2+} and Mg^{2+} can link the NZVI particle with HA, forming an NZVI−metal−HA complex that can significantly enhance adsorption (*39*). These results are informative for water treatment using NZVI because of the coexistence of competing anions and divalent cations in groundwater.

SEM and XRD Observations: Long-Term Study. We investigated the long-term effect of HA (500 mg L^{-1}) adsorption on NZVI (25 g L^{-1}) collected after reaction for 1, 30, 60, and 90 days. Corresponding FE-SEM images show the different surface textures and different pore sizes with respect to time of adsorption and precipitation of HA onto NZVI. Platelike structures (Figure 5a) were formed when NZVI reacted with HA for 1 day, and the morphology slowly

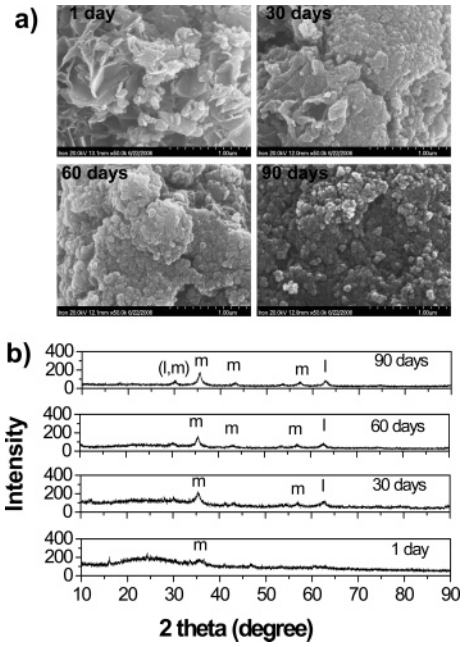

FIGURE 5. FE-SEM images of (a) HA treated NZVI and (b) XRD at 1, 30, 60, and 90 days. 500 mg L^{-1} HA reacted with 50 g L^{-1} NZVI in 0.01 M NaCl at 25 °C. XRD measured peaks are due to magnetite−maghemite (m) (Fe_3O_4/γ-Fe_2O_3) and lepidocrocite (l) (γ-FeOOH).

changed, as there were an increased number of round-shaped structures at 30 and 60 days, until at 90 days all the structures had changed.

SEM images showed that the very thin NZVI layer disappeared over time, replaced with the more stable round-shaped structures, following the Gay−Lussac−Oswald ripening rule (*14*). At the same time, corresponding XRD data analyses show that after 1 day Fe^0 was absent and a new peak of maghemite (m) appeared (Figure 5b). After 30 days, more peaks of different iron oxide/hydroxides such as maghemite−magnetite (m) (Fe_3O_4/γ-Fe_2O_3) and lepidocrocite (γ-FeOOH) appeared (*40*), and these peaks continuously increased in number and size from 60 to 90 days. This is one of the first reports that clearly illustrates the possible structural and crystalline change occurring on NZVI when it is treated with HA for up to 3 months.

Figure S4 (Supporting Information) analyzed by SEM-EDX shows the changes which occurred in the elemental composition of HA-treated NZVI at 1, 30, 60, and 90 days. Atomic weight-based quantitative SEM-EDX peak area analysis shows untreated NZVI having Fe:O ≡ 85:13.5. Note that the elemental composition changed to Fe:O:C ≡ 58:29:12 after reaction with HA for 1 day. This % atomic ratio further changed to Fe:O:C ≡ 49:36:13.5, Fe:O:C ≡ 35:48:22, and Fe:O:C ≡ 31:52:17 for 30, 60, and 90 days, respectively. This change illustrates that the presence of C increased with an increase of reaction time from 1 to 60 days and decreased at 90 days. Conversely, the amount of Fe decreased continuously up to 90 days, whereas the O content increased. These changes in elemental composition suggest that complexation of HA with NZVI decreased after 60 days and that the formation of oxy-hydroxide continuously occurred as time increased from 1 to 90 days. This finding may be significant for predicting the long-term effect of HA onto NZVI when considering direct injection of NZVI in the soil system to create a mobile reactive zone to remediate different contaminants, where HS is required to coexist (*15*, *20*, *41*).

Effect of HA on Kinetics of Arsenic Removal. Figure 6 shows the removal of 2 mg L^{-1} As(III) and As(V) in the absence and presence of HA, respectively, at 0.3 g L^{-1} NZVI and initial pH 6.5. Here, the surface normalized rate constant (k_{sa}) for

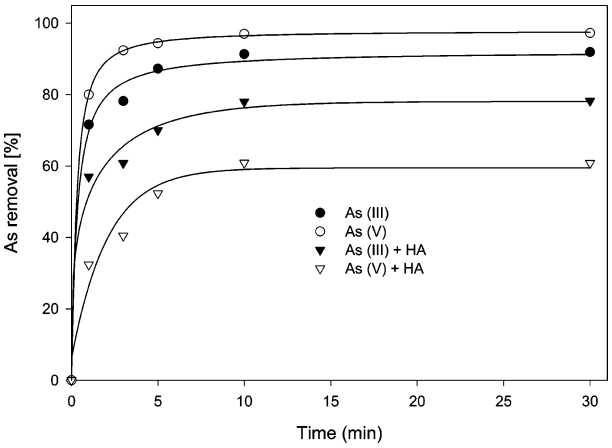

FIGURE 6. Effect of HA on the adsorption kinetics of As(III) and As(V) using NZVI. Reaction conditions: 2 mg L^{-1} As(III) and As(V), 20 mg L^{-1} HA, 0.3 g L^{-1} NZVI, and pH 6.5.

As(III) and As(V) were 1005 and 1440 mL m^{-2} h^{-1}, respectively, which were reduced by 43% for As(III) and 68% for As(V) in the presence of 20 mg L^{-1} HA, and became 578 and 459 mL m^{-2} h^{-1}, respectively (Table S1). The observed reduction of surface-normalized rate constants (k_{sa}) may have resulted from the following factors: (1) the occupation or obstruction of a large proportion of sorption sites by HA; (2) slowing the rate at which arsenic species encountered favorable sites; (3) the coagulation of NZVI by HA, further diminishing the number of available surface sites; and (4) the reduction of corrosion rates of NZVI by HA, which in turn reduces the formation of new sorption sites of arsenic (*42*). However, this phenomenon could be quite important in an arsenic treatment process using NZVI, as the total removal efficiency is reduced in the presence of HA.

Implications for HA and Arsenic Remediation. Our results present a detailed investigation of HA and NZVI interaction and groundwater chemistry (anion and cation) effect, of great significance in water treatment as HA abundantly coexists in groundwater with arsenic and other pollutants. It was determined that HA can be completely removed by NZVI at several different pH values. Furthermore, the results of this study demonstrate that HA has competitive effects with groundwater pollutants such as arsenic, and these effects should be considered during the application of adsorbents such as NZVI for groundwater remediation. In addition, we have demonstrated this competitive effect during the remediation of As(III) and As(V), which opens up further possibilities for competition with other groundwater pollutants.

We have presented evidence that 20 mg L^{-1} HA could reduce the surface normalization rate constant (k_{sa}) of 2 mg L^{-1} As(III) and As(V) from 100% to 43% and 68%, respectively. However, the HA concentrations used in these experiments are relatively high, and the negative effects of HA on arsenic adsorption on NZVI should generally be smaller in the field. For successful field applications of long-term in-situ and ex-situ groundwater treatments using NZVI, a more detailed study of surface reactions of NZVI with a variety of dissolved pollutants in the presence of HA should be further undertaken.

Acknowledgments

This work was supported by a grant from the National Research Laboratory Program by the Korea Science and Engineering Foundation.

Supporting Information Available

A table and four figures showing additional details of our analysis. This material is available free of charge via the Internet at http://pubs.acs.org.

Literature Cited

(1) Sparks, D. L. *Environmental Soil Chemistry*; Academic Press: San Diego, CA, 1995.

(2) Wall, N. A.; Choppin, G. R. Humic acids coagulation: influence of divalent cations. *Appl. Geochem.* **2003**, *18*, 1573−1582.

(3) Bai, R.; Zhang, X. Polypyrrole-coated granules for humic acid removal. *J. Colloid Interface Sci.* **2001**, *243*, 52−60.

(4) Schmitt, D.; Saravia, F.; Frimel, F. H.; Schuessle, W. NOM-facilitated transport of metal ions in aquifers: importance of complex-dissociation kinetics and colloid formation. *Water Res.* **2003**, *37*, 3541−3550.

(5) Yuan, W.; Zydney, A. L. Humic acid fouling during ultrafiltration. *Environ. Sci. Technol.* **2000**, *34*, 5043−5050.

(6) Tratnyek, P. G.; Scherer, M. M.; Deng, B.; Hu, S. Effects of natural organic matter, anthropogenic surfactants, and model quinones on the reduction of contaminants by zero- valent iron. W*ater Res.* **2001**, *35*, 4435−4443.

(7) Klausen, J.; Vikesland, P. J.; Kohn, T.; Burris, D. R.; Ball, W. P.; Roberts, A. L. Longevity of granular iron in groundwater treatment processes: solution composition effects on reduction of organohalides and nitroaromatic compounds. *Environ. Sci. Technol.* **2003**, *37*, 1208−1218.

(8) Kaneco, S.; Itoh, K.; Katsumata, H.; Suzuki, T.; Masuyama, K.; Funasaka, K.; Hatano, K.; Ohta, K. Removal of natural organic polyelectrolytes by adsorption onto tobermorite. *Environ. Sci. Technol.* **2003**, *37*, 1448−1451.

(9) Bernand, S.; Chazal, Ph.; Mazet, M. Removal of organic compounds by adsorption on pyrolusite (β-MnO_2). *Water Res.* **1997**, *31*, 1216−1222.

(10) Davis, A. P.; Bhatnagar, V. Adsorption of cadmium and humic acid onto hematite. *Chemosphere* **1995**, *30*, 243−256.

(11) Wang, L.; Chin, Y.; Traina, S. J. Adsorption of (poly)maleic acid and an aquatic fulvic acid by goethite. *Geochim. Cosmochim. Acta* **1997**, *61*, 5313.

(12) Avena, M. J.; Koopal, L. K. Kinetics of humic acid adsorption at solid-water interfaces. *Environ. Sci. Technol.* **1999**, *33*, 2739.

(13) Gu, B.; Schmitt, J.; Chen, Z.; Liang, L.; McCarthy, J. F. Adsorption and desorption of natural organic matter on iron oxide: mechanisms and models. *Environ. Sci. Technol.* **1994**, *28*, 38−46.

(14) Kanel, S. R.; Manning, B.; Charlet, L.; Choi, H. Removal of arsenic-(III) from groundwater by nanoscale zero-valent iron. *Environ. Sci. Technol.* **2005**, *39*, 1291−1298.

(15) Kanel, S. R.; Greneche, J. M.; Choi, H. Arsenic(V) removal from groundwater using nano scale zero-valent iron as a colloidal reactive barrier material. *Environ. Sci. Technol.* **2006**, *40*, 2045−2050.

(16) Wang, C. B.; Zhang, W. X. Synthesizing nanoscale iron particles for rapid and complete dechlorination of TCE and PCBs. *Environ. Sci. Technol.* **1997**, *31*, 2154−2156.

(17) Song, H.; Carraway, E. R. Reduction of chlorinated ethanes by nanosized zero-valent iron: kinetics, pathways, and effects of reaction conditions. *Environ. Sci. Technol.* **2005**, *39*, 6237−6245.

(18) Ponder, S. M.; Darab, J. G.; Mallouk, T. E. Remediation of Cr(VI) and Pb(II) aqueous solutions using supported, nanoscale zero-valent iron. *Environ. Sci. Technol.* **2000**, *34*, 2564−2569.

(19) Yang, G. C. C.; Lee, H. Chemical reduction of nitrate by nanosized iron: kinetics and pathways. *Water Res.* **2005**, *39*, 884−894.

(20) Zhang, W.-X. Nanoscale iron particles for environmental remediation: An overview. *J. Nanopart. Res.* **2003**, *5*, 323−332.

(21) Swartz, C. H.; Blute, K. N.; Badruzzaman, B.; Ali, A.; Brander, D.; Jay, J.; Besancon, J.; Islam, S.; Hemond, F. H.; Harvey, F. C. Mobility of arsenic in a Bangladesh aquifer: Inferences from geochemical profiles, leaching data, and mineralogical characterization. *Geochim. Cosmochim. Acta* **2004**, *68*, 4539−4557.

(22) Nurmi, J. T.; Tratnyek, P. G.; Sarathy, V.; Baer, D. R.; Amonette, J. E.; Pecher, K.; Wang, C.; Linehan, J. C.; Matson, D. W.; Penn, R. L.; Driessen, M. D. Characterization and properties of metallic iron nanoparticles: spectroscopy, electrochemistry, and kinetics. *Environ. Sci. Technol.* **2005**, *39*, 1221−1230.

(23) Dries, J.; Bastiaens, L.; Springael, D.; Kuypers, S.; Agathos, S. N.; Diels, L. Effect of humic acids on heavy metal removal by zero-valent iron in batch and continuous flow column systems. *Water Res.* **2005**, *39*, 3531−3540.

(24) Deng, S.; Bai, R. B. Aminated polyacrylonitrile fibers for humic acid adsorption: behaviors and mechanisms. *Environ. Sci. Technol.* **2003**, *37*, 5799−5805.

(25) Illies, E.; Tombácz, E. The effect of humic acid adsorption on pH-dependent surface charging and aggregation of magnetite nanoparticles. *J. Colloid Interface Sci.* **2006**, *295*, 15−123.

(26) Filius, J. D.; Lumsdan, D. G.; Meeussen, J. C. L.; Hiemstra, T.; Riemsdijk, W. H. V. Adsorption of fulvic acid on goethite. *Geochim. Cosmochim. Acta* **2000**, *64*, 51−60.

(27) Gu, B.; Schmitt Chen, Z.; Liang, L.; McCarthy, J. F. Adsorption and desorption of different organic matter fractions on iron oxide. *Geochim. Cosmochim. Acta* **1995**, *59*, 219−229.

(28) IHSS. http://www.ihss.gatech.edu/(accessed June 11, 2006).

(29) Fu, H.; Quan, X. Complexes of fulvic acid on the surface of hematite, goethite, and akaganeite: FTIR observation. *Chemosphere* **2006**, *63*, 403−410.

(30) Xie, L.; Shang, C. Role of humic acid and quinone model compounds in bromate reduction by zero-valent iron. *Environ. Sci. Technol.* **2005**, *39*, 1092−1100.

(31) Cho, Jaeweon. Natural organic matter (NOM) reflection by, and flux-decline of, nanofiltration (NF) and ultrafiltration (UF) membrane. Ph.D. Thesis, University of Colorado at Boulder, 1998.

(32) Ali, M. A.; Dzombak, D. A. Competitive sorption of simple organic acids and sulfate on goethite. *Environ. Sci. Technol.* **1996**, *30*, 1061−1071.

(33) Geelhoed, J. S.; Hiemstra, T.; Van Riemsdijk, W. H. Competitive interaction between phosphate and citrate on goethite. *Environ. Sci. Technol.* **1998**, *32*, 2119−2123.

(34) Guan, X. H.; Shang, C.; Chen, G. H. Competitive adsorption of organic matter with phosphate on aluminum hydroxide. *J. Colloid Interface Sci.* **2006**, 296, *1*, 51−58.

(35) Peng, X.; Luan, Z.; Chen, F.; Tian, B.; Jia, Z. Adsorption of humic acid onto pillared bentonite. *Desalination* **2005**, *174*, 135−143.

(36) Mylon, S. E.; Chen, K. L.; Elimelech, M. Influence of natural organic matter and ionic composition on the kinetics and structure of hematite colloid aggregation: implications to iron depletion in estuaries. *Langmuir* **2004**, *20*, 9000−9006.

(37) Xie, L.; Shang, C. The effects of operational parameters and common anions on the reactivity of zero-valent iron in bromate reduction. *Chemosphere*, **2007**, *66*, 1652−1659.

(38) Su, C.; Puls, R. W. Nitrate reduction by zerovalent iron: effects of formate, oxalate, citrate, chloride, sulfate, borate, and phosphate. *Environ. Sci. Technol.* **2004**, *38*, 2715−2720.

(39) Murphy, E. M.; Zachara, J. M.; Smith, S. C. Influence of mineral-bound humic substances on the sorption of hydrophobic organic compounds. *Environ. Sci. Technol.* **1990**, *24*, 1507.

(40) Manning, B. A.; Hunt, M. L.; Amrhein, C.; Yarmoff, J. A. Arsenic-(III) and arsenic(V) reactions with zerovalent iron corrosion products. *Environ. Sci. Technol.* **2002**, *36*, 5455−5461.

(41) Elliott, D. W.; Zhang, W. X. Field assessment of nanoscale bimetallic particles for groundwater treatment. *Environ. Sci. Technol.* **2001**, 35, 4922−4926.

(42) Redman, A. D.; Macalady, D. L.; Ahmann, D. Natural organic matter affects arsenic speciation and sorption onto hematite. *Environ. Sci. Technol.* **2002**, *36*, 2889−2896.

Received for review July 12, 2006. Revised manuscript received October 27, 2006. Accepted November 1, 2006.

ES0616534